Chinese Chemical Letters 34 (2023) 107931

Contents lists available at ScienceDirect

Chinese Chemical Letters

journal homepage: www.elsevier.com/locate/cclet

Photocatalytic thin film composite forward osmosis membrane for mitigating organic fouling in active layer facing draw solution mode

Yang Hu[a], Pin Zhao[a,*], Hao Liu[a], Xiawen Yi[a], Weilong Song[a], Xinhua Wang[a,b,*]

[a] Jiangsu Key Laboratory of Anaerobic Biotechnology, School of Environmental and Civil Engineering, Jiangnan University, Wuxi 214122, China
[b] Jiangsu Collaborative Innovation Center of Technology and Material of Water Treatment, Suzhou University of Science and Technology, Suzhou 215009, China

ARTICLE INFO

Article history:
Received 2 August 2022
Revised 13 October 2022
Accepted 18 October 2022
Available online 22 October 2022

Keywords:
Forward osmosis
Photocatalysis
Membrane orientation
Membrane fouling
Water permeation

ABSTRACT

As a high-flux operation mode of thin film composite-forward osmosis (TFC-FO) membrane, active layer facing draw solution (AL-DS) mode suffers from the severe membrane fouling tendency, which is not addressed well. Here, we introduced a photocatalyst (Anatase titanium dioxide, A-TiO_2) onto the support layer of TFC-FO membrane *via* the bonding of polydopamine (PDA) and polytetrafluoroethylene (PTFE), and prepared two photocatalytic membranes, A-TiO_2/PDA@TFC and A-TiO_2/PTFE@TFC. Compared with the pristine TFC-FO membrane, both A-TiO_2/PDA @TFC and A-TiO_2/PTFE@TFC had an improved water permeability (10.5 L $m^{-2}h^{-1}$ and 9.5 L m^{-2} h^{-1}, respectively) and reduced reverse NaCl flux salt (0.8 g m^{-2} h^{-1} and 0.7 g m^{-2} h^{-1}, respectively) in the AL-DS mode using 1 mol/L NaCl as draw solution and pure water as feed solution. Moreover, in the 16 h fouling experiment using 200 ppm bovine serum albumin (BSA) solution as a representative pollutant, the flux decline rate of both photocatalytic membranes was dramatically alleviated from 39.7% and 21.7% in the darkness to 8.5% and 9.7% under UV irradiation, respectively, indicating a significant anti-fouling capacity of photocatalytic effect. In all, the presence of A-TiO_2 endowed membrane with high permeability, high rejection efficiency and excellent anti-fouling capacity under UV spotlight. As bonding agent, PTFE provided the modified membrane with a high photocatalytic effect and high self-cleaning capacity, while PDA increased the membrane permeability and protected membrane against photocatalytic damage. This work provides a simple and feasible method to improve the anti-fouling capacity of TFC-FO membrane in AL-DS mode.

Water shortage and poor water quality are great challenges to the whole world [1,2]. High retention membrane technology including nanofiltration (NF), reverse osmosis (RO) and forward osmosis (FO) has aroused widespread attentions in water treatment owing to its stable effluent quality and high separation efficiency [3–7]. Among them, FO process is driven by the osmotic pressure difference between draw solution (DS) and feed solution (FS) separated by a semi-permeable membrane. Compared with the pressure-driven NF and RO processes, FO process occurs spontaneously with no/low hydraulic pressure, and has the advantages of low energy consumption and fouling tendency, presenting a very good prospect in the treatment of intractable wastewater with a high concentration of contaminants and a high fouling potential [8–11]. As a widely used FO membrane, thin film composite (TFC) membrane contains a dense active layer (AL) formed on a porous support layer (SL) [12,13]. Due to the asymmetric structure, there are two orientations of the TFC membrane in the FO process, *i.e.*, AL facing FS (AL-FS) and DS (AL-DS) [14,15]. With regard to the AL-FS mode, it has a low fouling tendency, high rejection efficiency, but relatively low water flux caused by the severe diluted internal concentration polarization [16–19]. Even though many studies have been done to improve the membrane permeability, this issue cannot be solved well because of the inherent trade-off effect [20–23]. As the other orientation, the AL-DS mode has a higher water flux, but suffers from severe membrane fouling owing to the rough SL and high initial flux [24,25]. The severe membrane fouling led to the few applications of AL-DS mode. Nevertheless, the AL-DS mode would be a feasible membrane orientation with a higher water flux if the membrane fouling of SL can be relieved efficiently. Until now, there are still very few related studies on alleviating SL fouling of TFC-FO membrane in the AL-DS mode.

As a low-energy and environmental-friendly technology, semiconductor photocatalytic process shows great potentials in water treatment and energy conversion [26–28]. To date, quantities of ultraviolet (UV)-responded photocatalysts have been applied

* Corresponding authors.
E-mail addresses: pinzhao@jiangnan.edu.cn (P. Zhao), xhwang@jiangnan.edu.cn (X. Wang).

https://doi.org/10.1016/j.cclet.2022.107931
1001-8417/

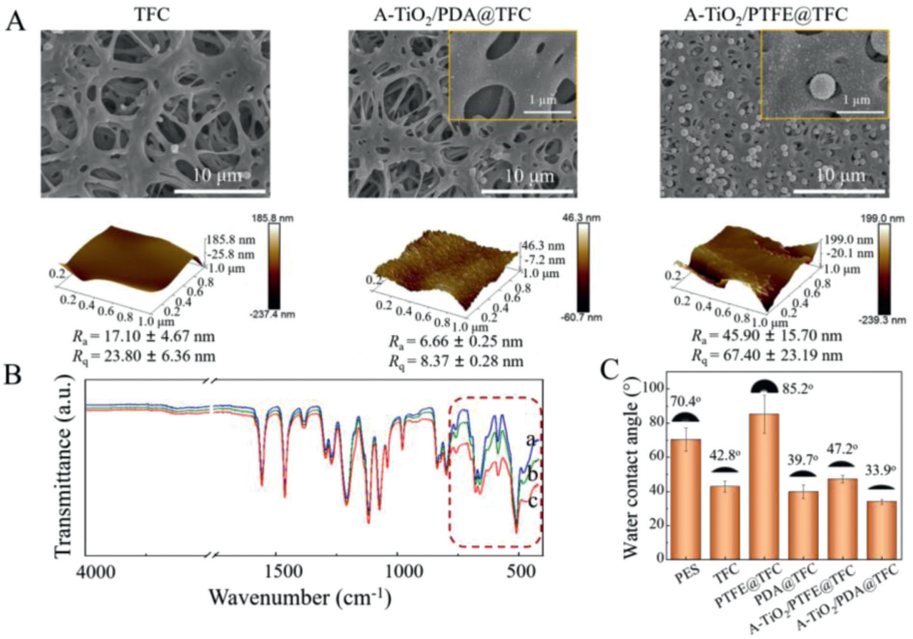

Fig. 1. SEM, AFM images and FT-IR curves of the SL of (A, B-a) TFC, (A, B-b) A-TiO_2/PDA@TFC and (A, B-c) A-TiO_2/PTFE@TFC membranes. (C) Water contact angles. The error bar represents the standard deviation of three independent repetitions.

to membrane technology, mainly focused on titanium dioxide (TiO_2), zinc oxide or their composites [29–34]. Especially, TiO_2 has been widely used for its high chemical stability, non-toxicity and low price [35–38]. For instance, a TiO_2-coated PES membrane was prepared by Lotfi *et al.* and showed high removal efficiency of steroid hormone when exposed to UV light with a continuous flow-through process [39]. Introducing photocatalysts into membrane material will well solve the problem of photocatalyst separation and recovery. Moreover, the confinement and enrichment effect of membrane will improve the photocatalytic efficiency [40]. Combining the interception and enrichment of membrane with photocatalytic degradation, the multifunctional membrane gains increasing concerns [41]. In this case, it is expected to mitigate the severe fouling of TFC-FO membrane in the AL-DS mode by introducing photocatalyst to the SL. The loaded photocatalysts would degrade the absorbed organic foulants, thus increasing the anti-fouling ability of SL. So far, studies on the fabrication of photocatalytic SL to migrate the membrane fouling of AL-DS mode have not been found in current literature.

In this work, for the first time, anatase-type TiO_2 (A-TiO_2) as photocatalyst was introduced onto the SL of TFC-FO membrane *via* two different bonding agents of polydopamine (PDA) and polytetrafluoroethylene (PTFE). The A-TiO_2 nanoparticles were well dispersed in the PDA and PTFE matrix and successfully loaded to the SL of TFC-FO membrane. Membrane morphology, properties, and performance in permeation and fouling experiment with and without UV illumination were investigated in the AL-DS mode of FO process. Compared to the control TFC membrane, both photocatalytic TFC-FO membranes based on PDA and PTFE had high permeability, low reverse NaCl flux and good anti-fouling ability. Our study presents an effective strategy to simultaneously enhance water flux and anti-fouling capacity of TFC-FO membrane for wastewater treatment.

As presented in Fig. S2 (Supporting information), the A-TiO_2/PDA@TFC and A-TiO_2/PTFE@TFC membranes were fabricated by introducing nanoparticles of A-TiO_2 to the back side of PES substrate using two methods based on PDA and PTFE, following the traditional interfacial polymerization (IP). The preparation process was referred to some previous works with some modifications [42,43]. The materials and chemicals used in this work were described in detail in Supporting information. Surface morphology of membranes were investigated by scanning electron microscopy (SEM, Zeiss Merlin Compact, Germany). As shown in Fig. 1A, TiO_2 nanoparticles were successfully coated on the PES substrate with the bonding of PDA and PTFE. Results of thermogravimetric analysis (TGA, Netzsch STA 449 F5, Germany) determined that the mass proportion of TiO_2 in A-TiO_2/PDA@TFC was about 16.5%, while that of A-TiO_2/PTFE@TFC was only 7.8% (Fig. S4 in Supporting information). The addition of PDA prevented the aggregation of TiO_2 and anchored TiO_2 onto PES evenly, in which the abundance catechol/quinone groups of PDA played a significant role [43]. Compared with A-TiO_2/PDA@TFC, A-TiO_2/PTFE@TFC had much more TiO_2 onto the PES surface, mainly due to the super hydrophobicity of PTFE [44]. Atomic force microscopy (AFM, Bruker Dimension Icon, USA) was used to evaluate the roughness of membrane surface, which was described in Fig. 1A. A-TiO_2/PDA@TFC ($R_a = 6.7$ nm) had a smoother SL, while A-TiO_2/PTFE@TFC ($R_a = 45.9$ nm) had a rougher SL than the original TFC membrane ($R_a = 17.1$ nm). As determined in attenuated total reflection flourier transformed infrared spectroscopy (ATR-FTIR, Thermo Scientific, Nicolet iS 10, USA) results (Fig. 1B), the characteristic peak of TiO_2 appeared at below 800 cm^{-1}, which indicated the successful coating of TiO_2 nanoparticles as well [45]. In addition, the water contact angle (Optical Contact Angle Meter, 15EC, Germany) was measured to evaluate the hydrophilicity of SL. As exhibited in Fig. 1C, the SL of original TFC membrane (42.8°) had a less contact angle than that of PES substrate (70.4°). It is well known that the polyamide layer formed in the other side of PES was more hydrophilic than the PES base. The presence of polyamide layer would promote the absorption of water droplets, making the contact angle value lower [46]. The hydroxyl and amino groups of PDA made the surface more hydrophilic (39.7°), while superhydrophobic PTFE coating led the surface less hydrophilic (85.2°). As a hydrophilic nanoparticle, the introduction of TiO_2 further enhanced the hydrophilicity of the membrane surface. The contact angles of A-TiO_2/PDA@TFC and A-TiO_2/PTFE@TFC was 33.9° and 47.2°, respectively. The enhancement of hydrophilicity was expected to improve the water flux and anti-fouling performance. The same characterization was conducted to

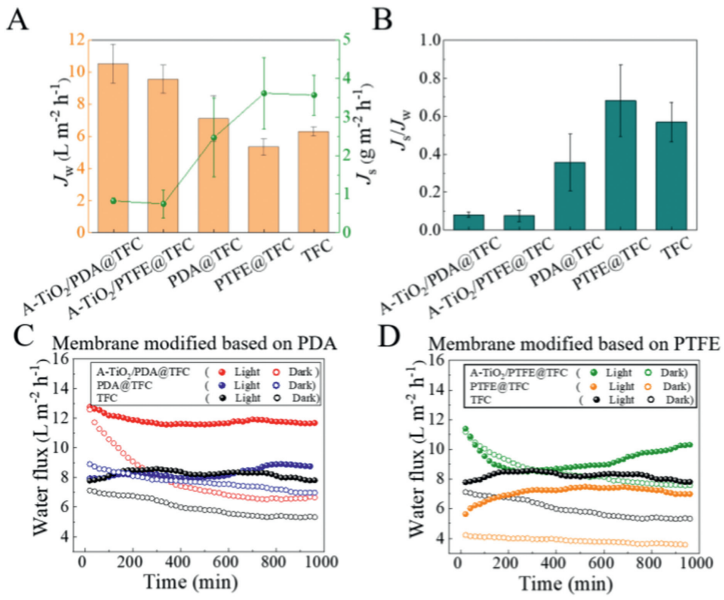

Fig. 2. (A) Water flux (J_w) and reverse salt flux (J_s), (B) J_s/J_w of different TFC-FO membranes in AL-DS mode using DI water (1 L) as FS and 1 mol/L NaCl (1 L) as DS. (C, D) Variation of membrane flux in fouling experiment using 200 ppm BSA (250 mL) as FS and 1 mol/L NaCl (1 L) as DS.

analyze the properties of AL (Figs. S7 and S8 in Supporting information). The AL of all membranes had similar surface morphologies and properties, indicating that the introduction of PDA, PTFE and A-TiO_2 had little influence on the IP process. More details of characterization measurement were provided in Supporting information.

The permeation performance and anti-fouling capacity of as-prepared FO membranes were evaluated in a lab-scale cross-flow filtration FO system with the membrane oriented in the AL-DS mode (Fig. S3 in Supporting information). Albumin from bovine serum (BSA) was selected as specific pollutant. The calculation of water flux (J_w) and reverse solute flux (J_s) was depicted in Eqs. S1 and S2 in Supporting information. Every experiment had been repeated at least three times. The water permeability and reverse salt flux of membranes were evaluated using 1 mol/L NaCl as DS and pure water as FS in the AL-DS mode. As shown in Fig. 2A, the water flux of original TFC membrane was 6.3 L m^{-2} h^{-1}, while that of PDA@TFC increased to 7.1 L m^{-2} h^{-1} and PTFE@TFC decreased to 5.3 L m^{-2} h^{-1}. The trend was consistent with the change of membrane surface hydrophilicity (Fig. 1C). After loading TiO_2, the water flux of A-TiO_2/PDA@TFC and A-TiO_2/PTFE@TFC significantly increased to 10.5 L m^{-2} h^{-1} and 9.5 L m^{-2} h^{-1}, respectively. On the other hand, except for PTFE@TFC (3.6 g $m^{-2}h^{-1}$), all the other modified TFC membranes had significant less reverse salt flux than the pristine TFC. The coating modification not only increased the water flux, but also decreased the reverse salt flux, in which the role of TiO_2 was particularly prominent. The value of J_s/J_w can exclude the effect of flux on the reverse salt flux, which would determine the salt interception capacity of membrane more accurately. As shown in Fig. 2B, compared with the pristine TFC, A-TiO_2/PTFE@TFC and A-TiO_2/PDA@TFC had a much lower J_s/J_w, indicating an enhanced membrane performance. Furthermore, the long-term permeation experiment of 96 h to estimate the stability of A-TiO_2/PDA @TFC and A-TiO_2/PTFE@TFC membrane. Results (Fig. S9 in Supporting information) presented that the water flux and reverse salt flux of both two membranes kept stable under long-term operating conditions. After the long-term experiment, the absorbance of feed solution and draw solution were measured by spectrophotometer (UV-1900i, Shimadzu, Japan) and no absorption peaks were detected (Fig. S10 in Supporting information). The long-time and stable operation and no leakage indicated the good stability of the modified membrane.

To evaluate the anti-fouling capacity of our prepared membrane under UV spotlight, the variation of water flux in fouling experiment was concluded in Figs. 2C and D. Water flux of TFC, PDA@TFC and PTFE@TFC membranes declined slowly by 21.8%, 20.5% and 15.5% during the fouling experiment in darkness, respectively. Unlike the condition of darkness, the permeation of these three membranes increased slightly under UV spotlight. It was mainly attributed to the enhanced temperature caused by photothermal effect (Fig. S11A in Supporting information). Compared with the membranes above, the water permeation of A-TiO_2/PDA@TFC and A-TiO_2/PTFE@TFC membranes were higher in the initial stage, but decreased faster in the dark fouling experiment. It indicated that A-TiO_2/PDA@TFC and A-TiO_2/PTFE@TFC suffered from a severe membrane fouling under the darkness. As we all know, the initial water flux has a critical impact on membrane fouling during FO process. It has been well reported that membrane fouling will be conspicuously intensified when the initial flux exceeds a certain critical value [47]. The severe membrane fouling would lead to a significant increase in the flux decline rate, 39.7% for A-TiO_2/PDA@TFC and 21.7% for A-TiO_2/PTFE@TFC, respectively. Under UV irradiation, both A-TiO_2/PDA@TFC and A-TiO_2/PTFE@TFC membranes had a less water flux decline (8.5% and 9.7%). The flux of A-TiO_2/PTFE@TFC with UV decreased in the first 200 min, but almost recovered to the initial value later. At the initial stage, the high initial water flux and less hydrophilic SL led to the severe membrane fouling, resulting in a sharp decrease of water permeation. After 200 min, the flux became low and membrane fouling reached a balance, the photocatalytic effect migrated membrane fouling through degrading foulants, leading to an increased flux. Moreover, the comparison of water flux between dark and lighting excluded the photothermal effect (Fig. S11B in Supporting information). Compared with the modified FO membranes reported recently, the A-TiO_2/PDA @TFC and A-TiO_2/PTFE@TFC membranes prepared in this study had high water flux, low reverse salt flux and excellent anti-fouling ability under UV illumination (Table S1 in Supporting information). In all, the modified TFC membrane based on A-TiO_2 showed a prominent permeation and anti-fouling performance under UV irradiation.

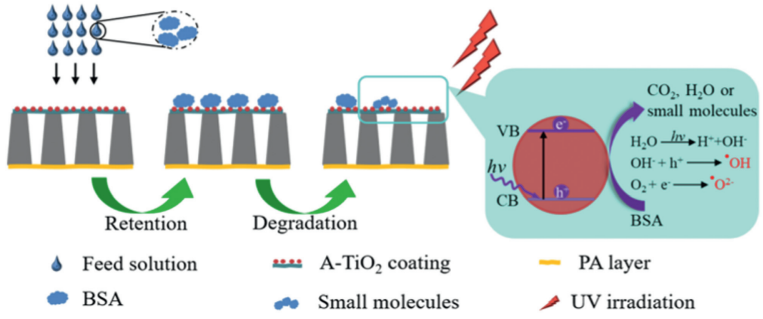

Fig. 3. Anti-fouling mechanism diagram of modified TFC-FO membranes under UV illumination in the AL-DS mode.

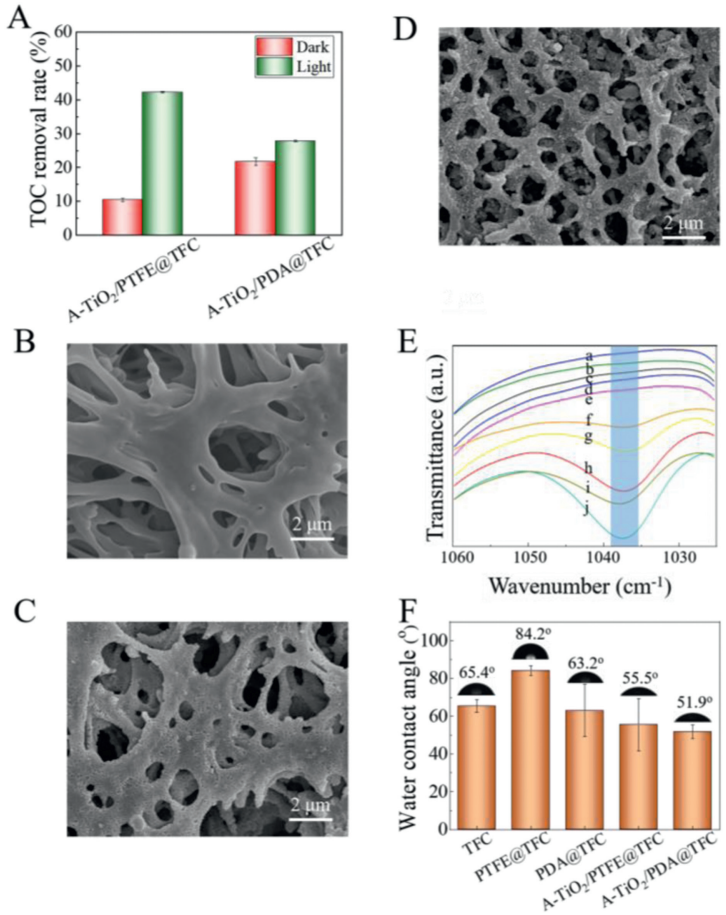

Fig. 4. (A) TOC removal of A-TiO_2/PTFE@TFC and A-TiO_2/PDA@TFC membranes under dark or light conditions. SEM micrographs of the supporting layer of (B) TFC, (C) A-TiO_2/PDA@TFC and (D) A-TiO_2/PTFE@TFC after 16 h illumination, (E) FT-IR curve of A-TiO_2/PTFE@TFC, PTFE@TFC, A-TiO_2/PDA@TFC and PDA@TFC in dark (a–e) and under illumination (f–j) within a certain wavenumber range, (F) contact angles of A-TiO_2/PTFE@TFC and A-TiO_2/PDA@TFC membranes. The error bar represents the standard deviation of three independent repetitions.

The anti-fouling mechanism of A-TiO_2/PDA@TFC and A-TiO_2/PTFE@TFC is shown in Fig. 3. In short, during the FO process in the AL-DS mode, BSA gathered and absorbed on the surface of PES substrate due to the membrane absorption and rejection. Then, the UV-responded A-TiO_2 generated strong oxidizing species and holes to degrade BSA into small molecule organics, or further degrade part of them into CO_2 and H_2O, achieving the purpose of mitigating membrane fouling.

Based on the conservation of materials, the decreased TOC in the feed bulk solution was caused by reverse diffusion, membrane adhesion and photocatalytic degradation, in which reverse diffusion could be ignored, due to the high rejection rate of TFC membrane towards BSA. To A-TiO_2/PTFE@TFC and A-TiO_2/PDA@TFC membranes operated under dark conditions, the decreased TOC in the bulk solution was mainly due to the membrane adhesion. While to these membranes under UV irradiation, the decreased TOC was attributed to the combined effect of membrane adhesion and photocatalytic degradation. To further determine the degradation capacity of A-TiO_2/PTFE @TFC and A-TiO_2/PDA@TFC membranes, the concentration of BSA at the corresponding FS was measured by a Total Organic Carbon analyzer (TOC-V CPH, Shimadzu Corporation, Japan) before and after fouling experiment with/without UV irradiation. The decreased TOC of the bulk solution in feed side was calculated according to the BSA concentration and FS volume (Eq. S3 in Supporting information), which was referred to TOC removal rate (Fig. 4A). The TOC removal rate of

A-TiO_2/PTFE@TFC and A-TiO_2/PDA@TFC membranes was 10.4% and 21.8% in the dark. Compared with A-TiO_2/PTFE@TFC, more BSA attached into the membrane surface of A-TiO_2/PDA@TFC. It indicated that A-TiO_2/PDA @TFC suffered from more severe membrane fouling in the dark, which was consistent with the results of water flux. The water flux of A-TiO_2/PDA@TFC was higher at the initial stage, but decreased faster than that of A-TiO_2/PTFE@TFC. The introduction of UV irradiation increased the TOC removal to both A-TiO_2/PTFE@TFC and A-TiO_2/PDA@TFC membranes. Unlike the dark condition, A-TiO_2/PTFE@TFC (42.3%) had a greater TOC removal rate than A-TiO_2/PDA@TFC (27.8%) under UV illumination. It implied that the A-TiO_2/PTFE@TFC membrane had a better photocatalytic effect, which could effectively mineralize the foulants adsorbed on the membrane surface. The relatively weak photocatalytic degradation ability of A-TiO_2/PDA@TFC membrane was probably attributed to the inhibitory effect of PDA on the photocatalytic effect of A-TiO_2 [48]. However, the water flux of A-TiO_2/PDA@TFC membrane maintained high in the fouling experiment under UV illumination. It might because that the fouling layer became loose due to the weak photocatalytic degradation of A-TiO_2/PDA, which had no apparent influence on membrane permeability. The SEM results in Fig. S12 (Supporting information) further verified our suggestion.

To further understand the photocatalytic effect of A-TiO_2/PDA@TFC and A-TiO_2/PTFE@TFC membrane, the substrate morphology and properties were investigated after UV irradiation. As shown in Fig. 4B, the UV illumination had no influence on the surface morphology of the SL to the membrane without photocatalysts loaded (Figs. S13A and B in Supporting information). However, it is clear that both the A-TiO_2/PDA@TFC and A-TiO_2/PTFE@TFC membranes were degraded to varying degrees (Figs. 4C and D). This might be attributed to the oxidative decomposition of the organic membrane by the strong oxidizing species produced by the photo-induced photocatalyst [48]. In addition, compared with A-TiO_2/PTFE@TFC, A-TiO_2/PDA@TFC suffered from less damaged, due to the inhibitory effect of PDA coating on the production and transfer of oxidizing species and holes [49,50]. Results of FT-IR measurement revealed that a new hydroxyl peak at 1033 cm^{-1} was produced to all membranes after UV irradiation (Fig. 4E), and the intensity varies in the rank of PDA@TFC > A-TiO_2/PDA@TFC > TFC > PTFE@TFC > A-TiO_2/PTFE@TFC. The contact angle of TFC membranes increased slightly after UV illumination, except for the PTFE@TFC (Fig. 4F). The introduction of hydroxyl did not lead to the enhancement of hydrophilicity, which can be explained by the decrease of amide III band after illumination (Fig. S14 in Supporting information). Furthermore, the peak intensity of PES substrate became weak after illumination, resulted from the aging of PES substrate during UV irradiation.

In this work, A-TiO_2 was successfully loaded onto the SL of TFC membranes with the bonding of PDA and PTFE, respectively. The as-prepared A-TiO_2/PDA@TFC and A-TiO_2/PTFE@TFC membranes exhibited a good stability and significantly improved performance compared with the pristine TFC membrane, mainly reflected in higher water flux (from 6.3 to 10.5 and 9.5 L m^{-2} h^{-1}, respectively) and lower reverse salt flux (from 3.6 to 0.8 and 0.7 g m^{-2} h^{-1}, respectively). Moreover, in the fouling experiments, both membranes exhibited extraordinary antifouling performance with a low flux decline of 8.5% and 9.7% under UV illumination. With hydrophilic PDA and more A-TiO_2 loading, A-TiO_2/PDA@TFC had excellent hydrophilicity and better flux performance, so as to obtain higher water production efficiency. However, PDA as a free radical scavenger could not only prevent the degradation of the PES substrate, but also inhibit the photocatalytic effect of A-TiO_2. In addition, less A-TiO_2 were loaded on the surface of A-TiO_2/PDA@TFC, leading to a poor degradation effect under UV, although the small molecular organics produced by its degradation would not significantly affect the water flux. In contrast, in spite the introduction of PTFE and less TiO_2 loading resulted to a relatively low flux, many A-TiO_2 loaded on the membrane surface provided A-TiO_2/PTFE@TFC membrane with an excellent photocatalytic effect under UV. Without the limitation of free radical scavenger, the membrane fouling had been well alleviated, but the PES substrate was damaged slightly. This work revealed a novel thread to relieve the severe organic fouling of TFC-FO membranes in the AL-DS mode *via* applying photocatalysts.

Declaration of competing interest

The authors declare that they have no known competing financial interests or personal relationships that could have appeared to influence the work reported in this paper.

Acknowledgements

This work was supported by the National Natural Science Foundation of China (Nos. 52100089 and 51978312), the Six Major Talent Peaks of Jiangsu Province (No. 2018-JNHB-014), and Youth Fund of Basic Research Program of Jiangnan University (No. JUSRP121058).

Supplementary materials

Supplementary material associated with this article can be found, in the online version, at doi:10.1016/j.cclet.2022.107931.

References

[1] R.F. Service, Science 313 (2006) 1088–1090.
[2] M. Elimelech, W.A. Phillip, Science 333 (2011) 712–717.
[3] L.D. Nghiem, A.I. Schäfer, M. Elimelech, Environ. Sci. Technol. 38 (2004) 1888–1896.
[4] M. Qasim, N.A. Darwish, S. Sarp, N. Hilal, Desalination 374 (2015) 47–69.
[5] K.P. Lee, T.C. Arnot, D. Mattia, J. Membr. Sci. 370 (2011) 1–22.
[6] N. Akther, A. Sodiq, A. Giwa, et al., Chem. Eng. J. 281 (2015) 502–522.
[7] B. Chanhee, W. Yunkun, Z. Ines, et al., Environ. Sci. Technol. 52 (2018) 7279–7288.
[8] S.E. Kwan, E. Bar-Zeev, M. Elimelech, J. Membr. Sci. 493 (2015) 703–708.
[9] S. Lee, C. Boo, M. Elimelech, S. Hong, J. Membr. Sci. 365 (2010) 34–39.
[10] E.W. Tow, D.M. Warsinger, A.M. Trueworthy, et al., J. Membr. Sci. 556 (2018) 352–364.
[11] Z.Y. Li, V. Yangali-Quintanilla, R. Valladares-Linares, et al., Water Res. 46 (2012) 195–204.
[12] Z. Yang, H. Guo, C.Y.Y. Tang, J. Membr. Sci. 590 (2019) 117297.
[13] D.L. Zhao, S. Japip, Y. Zhang, et al., Water Res. 173 (2020) 115557.
[14] S.F. Zhao, L.D. Zou, D. Mulcahy, J. Membr. Sci. 382 (2011) 308–315.
[15] G.T. Gray, J.R. McCutcheon, M. Elimelech, Desalination 197 (2006) 1–8.
[16] K. Lutchmiah, A.R.D. Verliefde, K. Roest, L.C. Rietveld, E.R. Cornelissen, Water Res. 58 (2014) 179–197.
[17] Y. Li, S.S. Zhao, L. Setiawan, L.Z. Zhang, R. Wang, J. Membr. Sci. 550 (2018) 163–172.
[18] J.R. McCutcheon, M. Elimelech, J. Membr. Sci. 284 (2006) 237–247.
[19] S. Phuntsho, S. Sahebi, T. Majeed, et al., Chem. Eng. J. 231 (2013) 484–496.
[20] S. Xiong, S. Xu, A. Phommachanh, M. Yi, Y. Wang, Environ. Sci. Technol. 53 (2019) 3331–3341.
[21] J. Wang, S. Zhang, P.F. Wu, et al., ACS Appl. Mater. Interfaces. 11 (2019) 12043–12052.
[22] H. Rho, S.J. Im, O. Alrehaili, et al., Environ. Sci. Technol. 55 (2021) 6984–6994.
[23] M. Xu, P. Zhao, C.Y. Tang, X. Yi, X. Wang, Chin. Chem. Lett. 33 (2022) 3818–3822.
[24] J. Kim, D. Suh, C. Kim, et al., Desalination 397 (2016) 157–164.
[25] L.F. Fang, L. Cheng, S. Jeon, et al., J. Membr. Sci. 552 (2018) 265–273.
[26] H. Kisch, Angew. Chem. Int. Ed. 52 (2013) 812–847.
[27] H. Tong, S.X. Ouyang, Y.P. Bi, et al., Adv. Mater. 24 (2012) 229–251.
[28] J. Li, Z. Lou, B. Li, Chin. Chem. Lett. 33 (2022) 1154–1168.
[29] K. Fischer, M. Grimm, J. Meyers, et al., J. Membr. Sci. 478 (2015) 49–57.
[30] N. Li, Y. Tian, J. Zhang, et al., J. Membr. Sci. 528 (2017) 359–368.
[31] Z. Lei, S. Xingxing, S. Meng, et al., ACS Appl. Mater. Interfaces. 13 (2021) 9975–9984.
[32] Z.W. Xu, T.F. Wu, J. Shi, et al., J. Membr. Sci. 520 (2016) 281–293.
[33] Y. Mansourpanah, S.S. Madaeni, A. Rahimpour, A. Farhadian, A.H. Taheri, J. Membr. Sci. 330 (2009) 297–306.
[34] S. Laohaprapanon, J. Matahum, L. Tayo, S.J. You, Taiwan Inst. Chem. Eng. 49 (2015) 136–141.
[35] Q. Zhang, Y. Xiao, L. Yang, et al., Chin. Chem. Lett. 34 (2023) 107628.

[36] C. Xiaobo, M.S. S, Chem. Rev. 107 (2007) 2891–2959.
[37] X. Chen, L. Liu, P.Y. Yu, S.S. Mao, Science 331 (2011) 746–750.
[38] Q. Guo, C.Y. Zhou, Z.B. Ma, X.M. Yang, Adv. Mater. 31 (2019) 1901997.
[39] S. Lotfi, K. Fischer, A. Schulze, A.I. Schafer, Nat. Nanotechnol. 17 (2022) 417.
[40] S. Leong, A. Razmjou, K. Wang, et al., J. Membr. Sci. 472 (2014) 167–184.
[41] W. Zhang, L. Ding, J. Luo, M.Y. Jaffrin, B. Tang, Chem. Eng. J. 302 (2016) 446–458.
[42] S.J. Ren, C. Boo, N. Guo, et al., Environ. Sci. Technol. 52 (2018) 8666–8673.
[43] R.X. Zhang, L. Braeken, P. Luis, X.L. Wang, B. Van der Bruggen, J. Membr. Sci. 437 (2013) 179–188.
[44] C. Chen, C. Du, D. Weng, et al., ACS Appl. Nano Mater. 1 (2018) 2632–2639.
[45] S.J. You, G.U. Semblante, S.C. Lu, R.A. Damodar, T.C. Wei, J. Hazard. Mater. 237 (2012) 10–19.
[46] Y. Li, S. Wang, H. Li, et al., J. Membr. Sci. 643 (2022) 120056.
[47] H. Wang, X. Wang, F. Meng, et al., J. Membr. Sci. 569 (2019) 41–47.
[48] H. Song, J. Shao, Y. He, B. Liu, X. Zhong, J. Membr. Sci. 405-406 (2012) 48–56.
[49] K. Feng, L. Hou, B.B. Tang, P.Y. Wu, J. Membr. Sci. 490 (2015) 120–128.
[50] H.Q. Wu, Y.J. Liu, L. Mao, et al., J. Membr. Sci. 532 (2017) 20–29.